SUPPORTING INFORMATION

Probing the redox states at the surface of electroactive nanoporous NiO thin films

Andrea G. Marrani[†]*, Vittoria Novelli[†], Stephen Sheehan°, Denis P. Dowling°, Danilo Dini[†]

[†]Department of Chemistry, "Sapienza" University of Rome, P.le Aldo Moro 5, Rome, Italy
°School of Mechanical and Materials Engineering, University College Dublin, Belfield, Dublin 4, Ireland

Table S1. Sampling depth values of Ni 2p and O 1s photoelectrons in NiO, collected at two different θ values excited by Mg Kα and Al Kα photons.

		X-ray source	
		Mg Kα	Al Kα
Orbital	θ (°)	Sampling depth, d (nm)*	
Ni 2p	11	2.8	3.8
	83	0.35	0.48
O 1s	11	4.2	5.2
	83	0.52	0.64

* d values for NiO are based on IMFPs calculated with TPP-2M equation using a density of 6.67 g cm^{-2} and a band gap of 4.3 eV (see ref. 1)

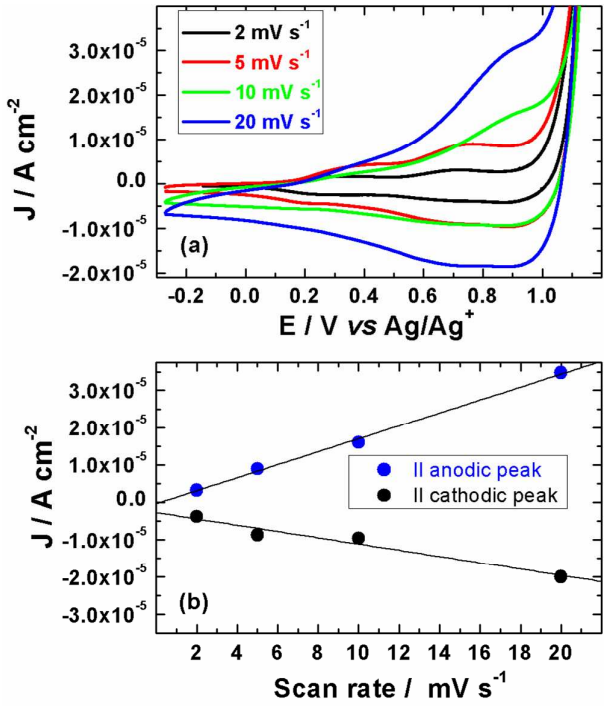

Figure S1. (a) Cyclic voltammograms of NiO (thickness: 0.2 μm) at various scan rates utilizing the same sample for all the rates. The experiments were executed with the order: 1) 2 mV s^{-1}; 2) 5 mV s^{-1}; 3) 10 mV s^{-1}; 4) 20 mV s^{-1}. Upon cycling there is a modification of the voltammograms due mainly to the change of the chemical composition of the electrode in aqueous electrolyte consisting in the progressive loss of coordinated water on the surface (see Eqn.1 in the Article). (b) Linear dependence of the amplitude of the second anodic and second cathodic peak of NiO (thickness: 0.2 μm) with the scan rate. Electrolyte: 0.2 M KCl, 0.01 M KH_2PO_4, 0.01 M Na_2HPO_4 in H_2O. Data extracted from Figure S1(a).

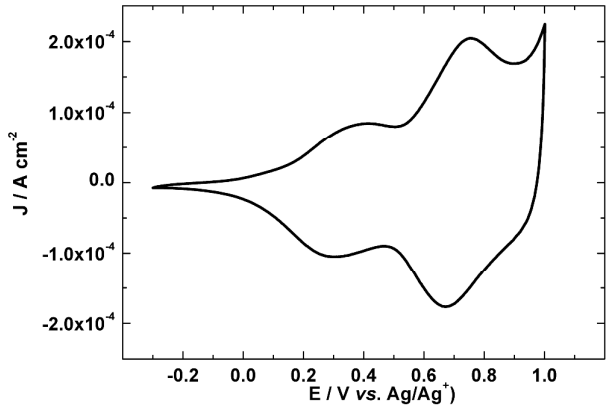

Figure S2. Cyclic voltammogram of the NiO sample (thickness: 2.5 μm) utilized for the chrono-amperometric experiments (*vide infra*) and XPS measurements. Scan rate: 10 mV s^{-1}; electrolyte: 0.2 M KCl, 0.01 M KH_2PO_4, 0.01 M Na_2HPO_4 in H_2O.

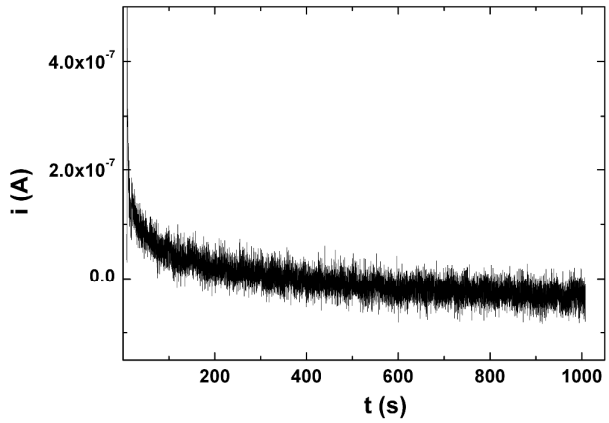

Figure S3. Chronoamperometric curve of NiO (thickness: 2.5 μm) polarized at 0.5 V *vs.* Ag/AgCl and successively analyzed with XPS. Electrolyte: 0.2 M KCl, 0.01 M KH_2PO_4, 0.01 M Na_2HPO_4 in H_2O.

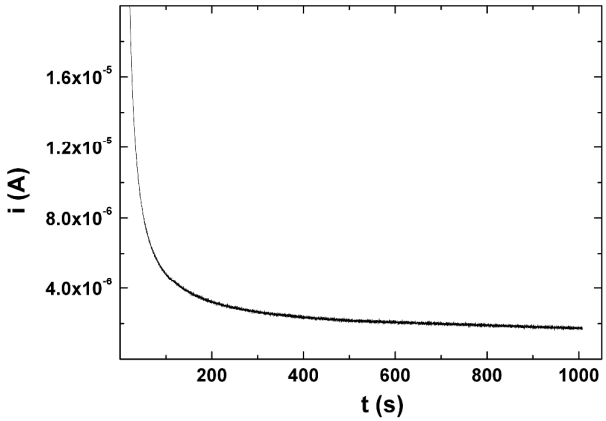

Figure S4. Chronoamperometric curve of NiO (thickness: 2.5 μm) polarized at 0.85 V *vs* Ag/AgCl and successively analyzed with XPS. Electrolyte: 0.2 M KCl, 0.01 M KH_2PO_4, 0.01 M Na_2HPO_4 in H_2O.

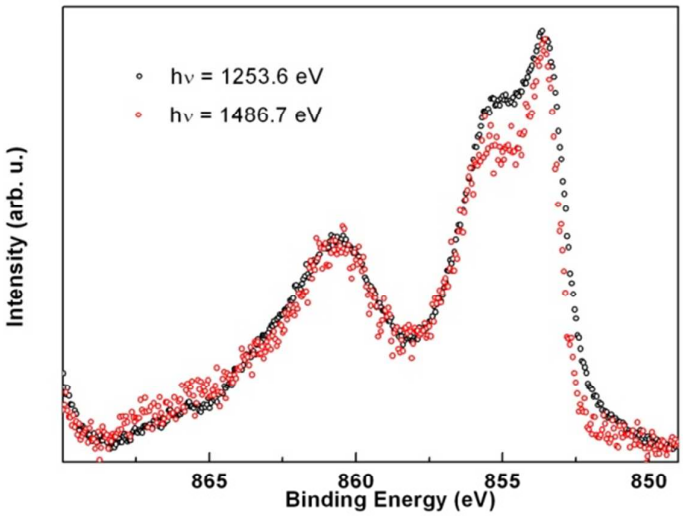

Figure S5. Comparison between experimental Ni $2p_{3/2}$ XP spectra of reference NiO sample, taken at $\theta = 73°$ with monochromatic Al Kα (red dots) and non-monochromatic Mg Kα (black dots) X-ray sources. Spectra were background-corrected and normalized at the intensity of the broad feature around 861 eV.

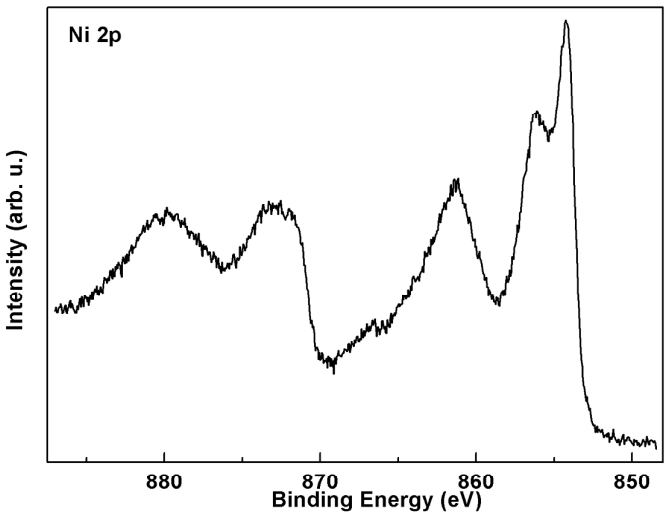

Figure S6. Whole-range experimental Ni 2p XP spectrum of reference NiO sample, taken with the monochromatic Al Kα X-ray source at $\theta = 11°$.

Additional comments on the state-of-art of theoretical simulations of Ni 2p XP spectrum.

The successful model of *non-local screening* has not been the only one so far reported to simulate the Ni 2p spectrum line shape in NiO. In fact, Sangaletti *et al.*[2,3] on the basis of a study of Ni 3s XP spectra in NiO and of Ni $2p_{1/2}$ spectra in La_2NiO_4, alternatively proposed that the electronic structure of NiO could be fully accounted for considering charge-transfer (CT), near degeneracy and exchange mechanisms. Another recent work[4] reported a theoretical configuration interaction (CI) calculation on a single-site NiO_6 cluster taking into account also the CT process between the so-called Zhang-Rice (ZR) doublet bound state at the top of the NiO valence band,[5-8] and the central metal ion. Such calculations revealed that the first ionization state in the Ni $2p_{3/2}$ spectrum (peak A, see full article) is of predominant $\underline{c}d^9\underline{Z}$ character (where $\underline{Z}$ represents a hole in the ZR doublet bound state), while the second feature (peaks B-C, see full article) has a $\underline{c}d^9\underline{L}$ character.

Auger parameter. An important contribution to the identification of the oxidation state of nickel in its oxides comes from the calculation of the modified Auger parameter[9] α' = BE + KE, where BE and KE are, in the present case, the binding energy of the Ni $2p_{3/2}$ photoelectrons and the kinetic energy of Auger electrons associated to the $L_3M_{4,5}M_{4,5}$ transition. The modified Auger parameter has the advantage that effects of charging and work function are cancelled out in its calculation, thus the obtained value is typical of a specific compound of the element under study. In our case, unfortunately, the calculation of α' suffers from errors due to surface speciation, because Ni $2p_{3/2}$ photoelectrons and Auger electrons are associated to different sampling depth, hence the procedure might not be very sensitive to the presence of topmost surface species. Anyhow, the truly surface-sensitive contribution of Ni $2p_{3/2}$ photoelectrons (d = 0.35 nm at θ = 83° with Mg Kα photon

source) is sufficient to render the estimation of α' indicative of possible chemical variations. In fact, the calculated values of α' for reference NiO, NiO0.5 and NiO0.85 samples with the Mg Kα photon source are 1697.8, 1698.8 and 1698.8, respectively. These values are fully compatible with the reported values for nickel oxide and oxyhydroxide.[10] As previously reported,[10,11] the ΔR value, a term representing the shift in relaxation energy involved in the core-hole decay between a zero-valent reference (*e.g.* Ni) and an n-valent compound (*e.g.* NiO), can be estimated by measuring the corresponding modified Auger parameter shift defined as $\Delta\alpha' = \Delta BE + \Delta KE$. It is assumed that $\Delta\alpha' \approx 2\Delta R$,[11] $\Delta BE = -\Delta\varepsilon - \Delta R$ and $\Delta KE = \Delta\varepsilon + 3\Delta R$,[12] where Δε represents the initial state effects, usually termed as "chemical shift". The evaluation of the initial (Δε) and final (ΔR) state effects via the calculation of Δα' resulted helpful in discriminating the nature of nickel oxides with different oxidation states.[10] In our case, such parameters were calculated for the three samples in the order of increasing oxidation state resulting in Δε values of -0.87, -2.1, -1.3 and ΔR values of -0.41, 0.044, 0.020, respectively, taking for Ni metal reference the data reported in ref. 10. The smaller Δε value of NiO compared to NiO0.5 (NiO0.85 being instead more similar to NiO) is indicative of the higher electron sharing and extent of covalent character in the former compound, due to the above mentioned charge transfer effects in the ground state. On the other hand, the ΔR value in NiO is considerably more negatively shifted compared to the oxyhydroxide species, where a nearly negligible effect is seen. Again, this implies that in the NiO sample a charge transfer mechanism, though probably to a lesser extent, is acting in the final state due to screening of the core-hole. Hence, the values of Δε and ΔR are here reported as a supporting evidence of a transition to oxyhydroxide species upon polarization of NiO sample at oxidative potentials.

Take-off angle dependence. In order to study the possible variations in the XP spectra of samples induced by the break of tridimensional bulk symmetry and chemical speciation at the surface, XP spectra were recorded both at high (surface-sensitive mode) and low (bulk-sensitive mode) take-off angles, θ. In Figure S7, a superposition of Ni $2p_{3/2}$ and O 1s spectra taken at $\theta = 11°$ and 83° are reported for the three samples analyzed. The overlapped Ni $2p_{3/2}$ spectra (left panel) were normalized equalizing the intensities of the broad feature at ~861 eV (peak D), which is insensitive to surface effects.[3,13] In the as-prepared NiO sample, the bulk and surface-sensitive spectra only differ within the 852-858 eV energy range, where surface effects are expected to play a relevant role. An increase of B/A and C/A peak area ratio is recorded at high θ values, such variations originating from a decrease in intensity of peak A (Table SI2). Such feature arises from the lowest-lying energy level in the core-ionized final state, with mainly $\underline{c}d^9\underline{L}$ character. Its intensity, associated to excitation processes at nickel sites within the bulk network of NiO_6 octahedra of NiO, decreases when a shallower portion of the surface is investigated. This is in agreement with a previous finding by Taguchi *et al*.[4]

In NiO0.5 sample the comparison between the spectra at the two θ values well evidences their different line shape, especially within the 852-858 eV energy range, due to chemical speciation at the surface upon electrochemical treatment at oxidative potentials. In fact, the two spectra can be assigned to two different species: the bulk-sensitive one to the underlying NiO, which is not affected by the electrochemical reaction upon polarization at 0.5 V since we have proved here that the electrochemical oxidation of NiO is surface-confined, and the surface-sensitive one to a thin layer of freshly formed β-NiOOH. Though the depth of analysis at $\theta = 83°$ is very small (0.35 nm),

the oxyhydroxide signal cannot be totally separated from that of NiO, because of effects induced by the high roughness of the nanostructured surface. In sample NiO0.85, the spectra superposition shows both a decrease of the lowest-lying main feature intensity and a slight variation in the line shape above 854 eV, with the peak maximum of the main feature shifted at higher BEs. Such variations from the bulk "pure" NiO features are hypothesized to be associated to the formation of a thin superficial layer of γ-NiOOH species, the considerations on the co-presence of a pure NiO signal still holding. Also for Ni0.85 sample the B/A and C/A peak area ratios have been calculated, utilizing the same NiO fitting parameter set for both angles. A decrease of the peak A intensity occurs in the surface-sensitive mode, again hinting at a predominance of ionization events confined at the surface.

The right panel of Figure S7 shows the overlap of O 1s spectra at the two θ values for the three samples. In the reference NiO sample a very slight difference is recorded, since the two spectra at θ = 11° and 83° overlap nearly perfectly. The surface enrichment of OH groups is then hardly detectable due to the surface roughness of the nanoporous sample. In sample NiO0.5 the presence of other components at the surface after electrochemical treatment is evident. In fact, though the hydroxide component hardly changes, the sizeable variation in lineshape is due to the presence of contributions associated to the buffering agent of the electrolyte solution and to interactions with alkali ions at low BE. Such modifications are also found in the NiO0.85 spectra with an even more pronounced difference between ~530 and ~534 eV. In this range an increased amount of hydroxide, water and buffering agent components is found in the spectrum at θ = 83°, denoting the surface confinement of these species. From the comparison of the Ni $2p_{3/2}$ spectra, the three samples show differences only within a few tenths of nm from the surface, confirming that the electrochemically-induced modifications are limited to such a very thin layer.

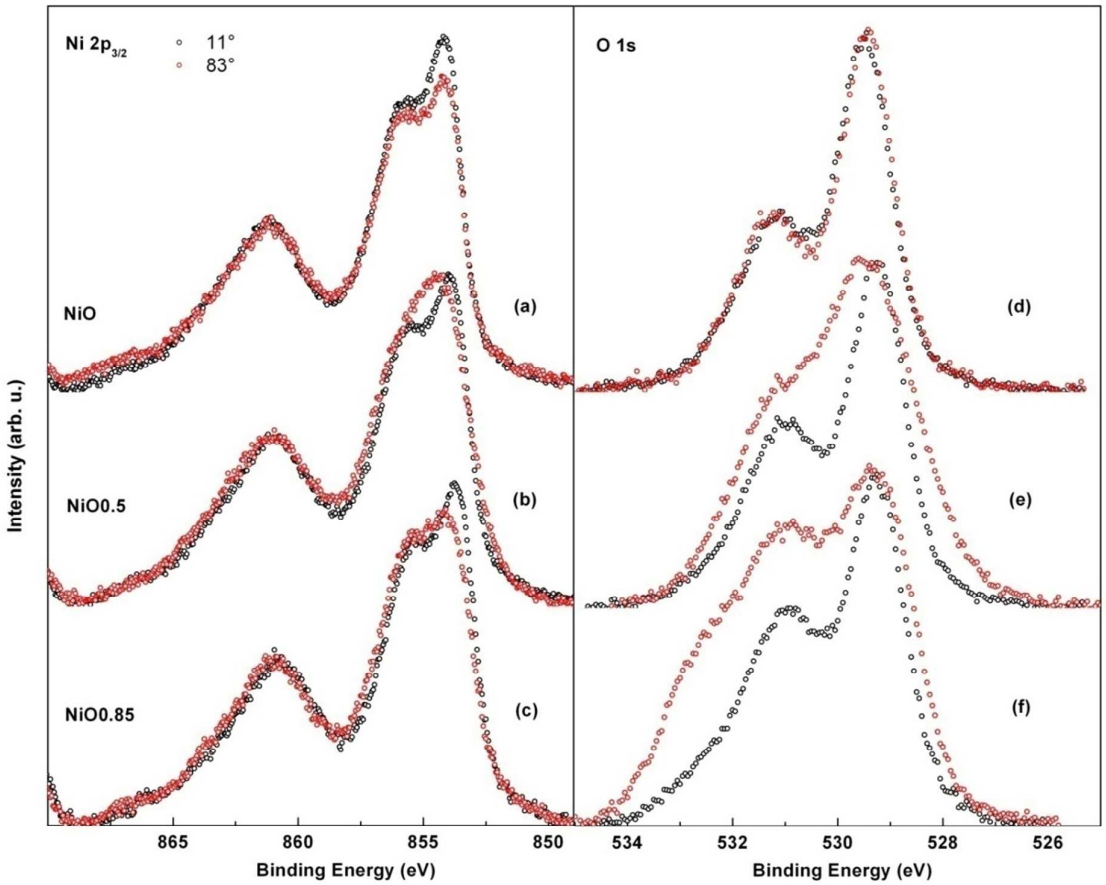

Figure S7. Ni $2p_{3/2}$ (a,b,c) and O 1s (d,e,f) XP experimental spectra of NiO (a,d), NiO0.5 (b,e) and NiO0.85 (c,f) samples recorded at take-off angles θ = 11° (black dots) and 83° (red dots) with the Mg Kα X-ray source.

Table S2. Ratios of the areas of the relevant peaks used in the fitting of the Ni $2p_{3/2}$ spectra of NiO and NiO0.85 samples[a,b] at the two different take-off angles (θ).

Sample	θ (°)	Peak B/Peak A	Peak C/Peak A
NiO	11	1.32	0.70
	83	1.45	0.86
NiO0.85	11	1.34	0.80
	83	1.58	0.89

[a] Values from NiO0.5 sample are not reported here since it has been fit to a different set of parameters. [b] Spectra were acquired with the Mg Kα X-ray source.

References

(1) Sawatzky, G. A.; Allen, J. W. *Phys. Rev. Lett*. **1984**, *53*, 2339–2342.
(2) Sangaletti, L.; Depero, L. E.; Parmigiani, F. Solid *State Commun.* **1997**, *103*, 421–424.
(3) Parmigiani, F.; Sangaletti, L. *J. Electron Spectrosc. Relat. Phenom.* **1999**, *98–99*, 287–302.
(4) Taguchi, M.; Matsunami, M.; Ishida, Y.; Eguchi, R.; Chainani, A.; Takata, Y.; Yabashi, M.; Tamasaku, K.; Nishino, Y.; Ishikawa, T.; Senba, Y.; Ohashi, H.; Shin, S. *Phys. Rev. Lett.* **2008**, *100*, 206401.
(5) Van Elp, J.; Eskes, H.; Kuiper, P.; Sawatzky, G. A. *Phys. Rev. B* **1992**, *45*, 1612-1622.
(6) Bala, J.; Oles, A. M.; Zaanen, J. *Phys. Rev. Lett.* **1994**, *72*, 2600–2603.
(7) Kuneš, J.; Anisimov, V. I.; Lukoyanov, A. V.; Vollhardt, D. *Phys. Rev. B* **2007**, *75*, 165115.
(8) Kuneš, J.; Anisimov, V. I.; Skornyakov, S. L.; Lukoyanov, A.V.; Vollhardt, D. *Phys. Rev. Lett.* **2007**, *99*, 156404.
(9) Wagner, C. D. *Faraday Discuss. Chem. Soc.* **1975**, *60*, 291–300.
(10) Biesinger, M. C.; Lau, L. W. M.; Gerson, A.; Smart, R. St. C. *Phys. Chem. Chem. Phys.* **2012**, *14*, 2434–2442.
(11) Moretti, G. *J. Electron Spectrosc. Relat. Phenom.* **1998**, *95*, 95–144.
(12) Wagner, C. D.; Taylor, J. A. *J. Electron Spectrosc. Relat. Phenom.* **1982**, *28*, 211–217.
(13) Alders, D.; Voogt, F.C.; Hibma, T.; Sawatzky, G. A. *Phys. Rev. B* **1996**, *54*, 7716–7719.